



Synthesis of Oil Palm Fronds Charcoal as Adsorbent to Reduce Levels of Fe (III) in Peat Water

Rahmat Zikri ^a, Evelin Natasyah ^a, Muhdarina ^{a,*}

^a Department of Chemistry, Faculty of Mathematics and Natural Sciences, University of Riau, Pekanbaru, Indonesia

*Corresponding author: muhdarina.m@lecturer.unri.ac.id

<https://doi.org/10.14710/jksa.25.8.300-306>



Article Info

Article history:

Received: 30th June 2022

Revised: 3rd October 2022

Accepted: 10th October 2022

Online: 12th October 2022

Keywords:

Charcoal; oil palm fronds; peat water

Abstract

The high content of carbon compounds in palm fronds (OPF) makes them potentially useful as an adsorbent. The carbonization method was used for the adsorbent synthesis process. This process began with collecting palm frond waste and then drying and sifting the adsorbent particle. This process resulted in the escape particles with a size of 80 mesh and suspended particles with 120 mesh. Then this process continued by carbonizing the palm fronds with temperature variations starting from (400, 500, and 600 °C) for 60 minutes to obtain Charcoal Oil Palm Fronds (COPF). The obtained COPF was determined for moisture and ash content and characterized using FTIR, XRD, and SEM to determine the surface, functional groups, degree of amorphism, crystallinity, and surface morphology. The adsorption efficiency of COPF was applied to the adsorption of Fe (III) in peat water under varying contact time, adsorbent mass, and peat water volume conditions. The water and ash content of COPF qualify the technical quality requirements for activated charcoal according to SNI 06-3730-1995. FTIR analysis detected the presence of vibrations of the C-O, O-H, C=O, C-C, and C-H functional groups on the COPF surface. The XRD pattern showed the existence of a semi-crystalline (002) and (100) plane structure, which is shown at scattering angles of $2\theta = 22^\circ$ and 42° . The surface morphology of COPF showed that as the carbonization temperature increased, the number of pores formed increased, and the pore size decreased. The best adsorption test results were obtained with a contact time of 30 minutes, an adsorbent mass of 1.00 g, and a peat water volume of 100 mL. The highest Fe adsorption efficiency was achieved by COPF 500, where the adsorbed mass was 0.054 mg. Increasing the carbonization temperature causes the water content to decrease and the ash content to increase. High water content and ash content cause a decrease in adsorption efficiency because they can cover the pores of the adsorbent.

1. Introduction

Oil palm (*Elaeis guineensis* Jacq.) is one of the industrial plants that play a critical role in producing cooking oil, fuel (biodiesel), soap products, and other oil-based products. Data from the Indonesian Central Statistics Agency shows that the area of Indonesian oil palm plantations in 2017 was 12.38 million ha and is estimated to continue to grow in 2018, covering an area of 12.76 million ha. The oil palm plantation area is spread over 25 provinces. Riau province has the largest oil palm plantation area, 2.21 million ha in 2017, and is estimated to increase in 2018 to 2.32 million ha [1]. The utilization of

oil palm fronds (OPF) is still not optimal. Palm fronds are only placed around oil palm trees or burned and used as plant fertilizer.

Palm fronds contain the three largest constituent compounds: cellulose (31.5%), hemicellulose (19.20%), and lignin (14%) [2]. The content of these organic compounds allows palm oil fronds to have the potential to be used as a material for making charcoal. This is because palm oil fronds have cellulose and lignin, which, when carbonized, produce charcoal due to incomplete combustion reactions [3].

The palm fronds waste has been converted into palm frond charcoal (Charcoal Oil Palm Fronds, COPF) with a calcination temperature of 600°C and a variation of 30, 60, and 120 minutes. The most significant efficiency of free fatty acid adsorption in CPO at COPF 600 at 60 minutes of carbonization time was 77.81% [4]. Research by Melati *et al.* [5] proves that activated carbon is effectively used as an adsorbent for solids, liquids, or gas. The results showed that activated carbon had a better performance than CNF in terms of ammonia adsorption ability.

The area of peatland in Indonesia is 1.46 million hectares, including Kalimantan (0.75 million hectares), Papua (0.40 million hectares), and Sumatra (0.31 million hectares). Oil palm plantations in Indonesia cover 8.90 million hectares, of which 1.25 million hectares are on peatland [2]. Riau is a province that has the largest peatland on the island of Sumatra, which is 4.04 million hectares. Water sources in peaty areas or swamp areas are generally shallow, with brown water and high levels of humus acid, organic matter, and iron. This type of water has characteristics such as dark brown to blackish (124–850 PtCo), high organic content (138–1560 mg/L KMnO₄), iron (Fe) content > 1 mg/L, manganese (Mn) content > 0.8 mg/L and acidic (pH 3.70–5.30) [6]. One method that can reduce the Fe content in peat water is the adsorption method.

Harfinda [7] synthesized a Ca-Alginate adsorbent that was applied to reduce the Fe content from the peat water. The most remarkable reduction efficiency of Fe content is 79.28% with optimum conditions of 0.75 g mass of adsorbent, 2 M CaCl₂, and 3 hours of adsorption. The adsorption efficiency of Fe from peat water is still relatively low; therefore, it is required to discover other sources, such as oil palm fronds waste, that are simple to find and prepare, environmentally friendly, time-efficient in decreasing Fe, and cost-effective.

From the explanation above, an adsorbent based on palm frond charcoal will be synthesized with carbonization temperature variations of 400, 500, and 600°C for 60 minutes based on Muhdarina *et al.* [4] and applied to the adsorption of Fe (III) in peat water based on Harfinda [7]. This research is expected to optimize local natural resources from oil palm frond biomass and to reduce Fe (III) levels from peat water.

2. Methods

This research used the carbonization method and explained the tools, materials, and synthesis steps below. The results of quantitative data were repeated three times.

2.1. Materials and equipment

The materials used in this study were oil palm fronds (OPF) obtained from Jl. Pekanbaru-Bangkinang KM 16 (0°27'NL and 101°21' WL), 1 M HNO₃ (98% nitric acid), buffer solution pH 4, 7, and 10 (Merck), distilled water, and demineralized water. The tools used in this study were a cooking knife, hotplate stirrer (Rexim RSH-1DR), analytical balance (ABJ 320-4NM reading accuracy: 0.1 mg/0.0001 g), oven (Heraeus Instruments), FTIR (IR

Prestige-21), SEM (6510 LA), AAS (AA-7000 Shimadzu), XRD (PANalytical Empyrean), pH meter (Hanna Instruments), furnace (Naberthem type L31 R), centrifuge (corning minicentrifuge), 80 and 120 mesh sieves, and laboratory glassware.

2.2. Preparation of COPF

The OPF was cut into a size range of ± 2 cm² before being cleaned with distilled water and then sun-dried to minimize its moisture content. The samples were further dried in a 105°C oven for two hours. Sample pieces were carbonized at different furnace temperatures (400, 500, and 600°C) for 60 minutes [5]. The carbonized samples were ground to a finer size, and then the results were homogenized by sifting through 80 and 120-mesh sieves. In order to remove water vapor from the air, the products were placed in a desiccator. The charcoal samples were labeled as COPF 400 (carbonization at 400°C for 60 minutes), COPF 500 (carbonization at 500°C for 60 minutes), and COPF 600 (carbonization at 600°C for 60 minutes).

2.3. Characterization of palm frond charcoal

2.3.1. Water content (SNI 06-3730-1995)

One gram of charcoal was put into a dry porcelain cup and oven-dried at 105°C for 2 hours. The dried charcoal was cooled in a desiccator and weighed to a constant. The water content can be calculated by equation (1).

$$\text{Water content (\%)} = \frac{a-b}{a} \times 100\% \quad (1)$$

where, a is the initial weight of charcoal (g), and b is the weight of dried charcoal (g).

2.3.2. Ash content (SNI 06-3730-1995)

Five grams of charcoal was placed in a crucible with a known weight and ashed in a furnace at 900 for an hour. The formed ash in the crucible was cooled and placed in a desiccator. The crucible was weighed until a constant weight was obtained. The ash content can be calculated by equation (2).

$$\text{Ash content (\%)} = \frac{\text{Ash weight (g)}}{\text{Sample weight (g)}} \times 100\% \quad (2)$$

2.3.3. Characterization of COPF

The COPF in KBr pellets was characterized using FTIR to identify the functional groups. The process of grinding COPF with KBr crystals (attempted in a dry state) was used to prevent the condensation of vapor from the atmosphere. The surface morphology of COPF was visualized using SEM. XRD was utilized to determine the degree of crystallinity by observing the peaks formed.

2.3.4. Peat water sampling

Samples of peat water were taken from irrigation in Rimbo Panjang village, Tambang district, Kampar regency, Riau. The procedure for collecting wastewater samples conforms to SNI 6989.59-2008, while the method for testing for iron (Fe) with AAS conforms to SNI 06-6989.4-2004. Sampling was conducted at three points: the surface, mid-depth, and bottom of the well. The pH of the peat water sample was determined in situ

before being transported to the lab, and HNO₃ was injected until the pH dropped below 2. A cooler was used to store the water sample.

2.3.5. Peat water adsorption

Adsorption was performed in batch experiments where 1 g adsorbent was added to 100 mL of peat water sample in an erlenmeyer flask and stirred using a hotplate stirrer at 120 rpm for different times of 15, 30, 45, and 60 minutes. Samples were centrifuged for 15 minutes at 6000 rpm, and the supernatants were pipetted to measure the Fe (III) content. This step determined the optimum adsorption time (step (a)).

Furthermore, the optimum time in step (a) was used as contact time at the adsorbent mass variation step with 0.5, 1, and 2 g. The experiment was carried out in action (a), and the optimum mass of the adsorbent was obtained in step (b). Then the results in steps (a and b) were used for volume variations of peat water of 100, 200, and 300 mL (step c). Then the Fe (III) levels were analyzed using (AAS). The amount of Fe(III) adsorbed was calculated by the equation below.

$$\text{Percent amount of Fe(III) (\%)} = (a - b) \times 100\% \quad (3)$$

where, a is the initial Fe weight of peat water (mg), and b is the weight of Fe after adsorption (mg).

3. Results and Discussion

3.1. Water content and ash content of COPF

The COPF characterization carried out in this study included an analysis of water and ash content. COPF, which has been synthesized by carbonization with different temperature variations of 400, 500, and 600°C for 60 minutes, was determined by water and ash content. Data on the water and ash content of COPF samples can be seen in Table 1.

Table 1. Water and ash content data of COPF adsorbent

Sample	Calcination temperature (°C)	Water content (%)	Ash content (%)
COPF 400	400	3.78	8.87
COPF 500	500	3.10	9.56
COPF 600	600	2.39	9.95
SNI 06-3730-1995		Max. 15	Max. 10

The COPF 400, COPF 500, and COPF 600 were analyzed gravimetrically for moisture and ash content. It is necessary to calculate the water content of an adsorbent to determine its hygroscopic properties. In Table 1, the water content of COPF 400, COPF 500, and COPF 600 were 3.78%, 3.10%, and 2.39%, respectively, indicating that the water content reduces as carbonization temperature increases. The decrease in water content as calcination temperature increases is caused by the increase in water in the vaporized COPF. The water content decreases with rising temperatures [8]. COPF400 achieved the highest water content of 3.78% due to the low carbonization temperature compared to other charcoals. Based on the technical quality requirements for activated charcoal

specified in SNI 06-3730-1995, COPF has been accepted as a standard adsorbent since its moisture content is less than the maximum permitted limit of 15%.

The ash content or total ash represents the total amount of minerals in the biomass. Ash content also indicates the number of metal oxides present in COPF. This ash was a residue of the combustion or carbonization process of the palm fronds. From Table 1, it can be seen that COPF ash content increased with increasing carbonization temperature, with COPF 400 at 8.87%, COPF 500 at 9.56%, and COPF 600 at 9.95%. This is because as the carbonization temperature rises, the metal has a higher possibility of oxidizing, producing a substantial amount of ash. Ash content increases with increased carbonization temperature [9]. COPF600 had the highest ash content of 9.95% due to its higher carbonization temperature than other charcoals. COPF has qualified the standard SNI 06-3730-1995 for the category of ash content for the technical quality requirement of activated charcoal, which is 10%.

3.2. Surface functional groups of COPF

Functional groups on the COPF surface were analyzed using the Fourier Transform Infrared Spectrophotometer (FTIR). The IR absorption spectra of the COPF sample are presented in Figure 1.

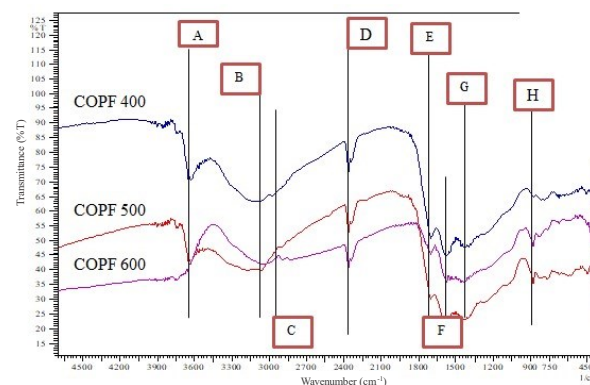


Figure 1. FTIR spectra for each temperature variation

Analysis of surface functional groups was necessary to determine the relationship between temperature variations and surface functional groups and the degradation of cellulose on the adsorbent's surface. Based on Figure 1, the spectra of the three synthesized samples generally showed the presence of O-H functional groups (phenol and free OH groups) at 3610-3670 cm⁻¹ (A). The stretching OH (carboxylate) at 3200-2800 cm⁻¹ (B) is probably the functional group of cellulose and adsorbed water. The 2924 cm⁻¹ (C), 2300-2400 cm⁻¹ (D), and 1600 cm⁻¹ (E) peaks are attributed to the C-H stretching, C-H bending, and C=C aromatic. In addition, the stretching C=O groups of carbonyls were found at 1800-1400 cm⁻¹ (F). These groups are regarded as functional groups in the chemical structure of hemicellulose and lignin. The absorption bands at 1200-1400 cm⁻¹ (G) correspond to CO (carboxylic acid). -CH rocking from cellulose appears at 896-900 cm⁻¹ (H) [10].

The appearance of aromatic C=C, CH, C=O carbonyl, and C-O is due to the presence of these functional groups on the surface of the charcoal, as well as the oxidation

process caused by heat, which forms O-H, C=O, and C-O groups. The functional groups on the surface of charcoal are generally phenol, ether, carboxyl, ketone, lactone, and anhydrous carboxylate [11].

The spectra of COPF 400, 500, and 600 share similarities, particularly at COPF 400 and 500, where the ranges are comparable. The difference was readily apparent when comparing COPF 400 and 500 to COPF 600. The difference in wavenumber 3610–3670 cm^{-1} , which corresponds to the O-H stretching vibration of the free O-H group, is most likely due to the functional group of cellulose or adsorbed water. As shown in Figure 1, the O-H stretching intensity of COPF 500 (3.648 cm^{-1}) was 40% lower than that of COPF 400 (3631 cm^{-1}), indicating that cellulose degradation occurred with increasing temperature. The intensity similarly decreased when examined from the perspective of the O-H stretch absorption at 3740 cm^{-1} (COPF 600). The increase in temperature causes the vibrational intensity of the functional groups to decline due to the degradation of the constituent compounds (cellulose, hemicellulose, and lignin) [12].

3.3. Crystallinity of COPF

Analysis using the XRD instrument was intended to determine the lattice parameters and degree of crystallinity by observing the peaks formed. The results of X-ray diffraction at COPF 400, COPF 500, and COPF 600 can be seen in Figure 2. The XRD showed two diffraction bands at $2\theta = 22\text{--}25^\circ$ and $42\text{--}44^\circ$. The peaks come from standard C graphite, which has crystalline properties. The amorphous phase in the diffractogram was characterized by a broad rise at $10\text{--}40^\circ$ [13]—determination of the degree of crystallinity of the sample using Origin Pro software.

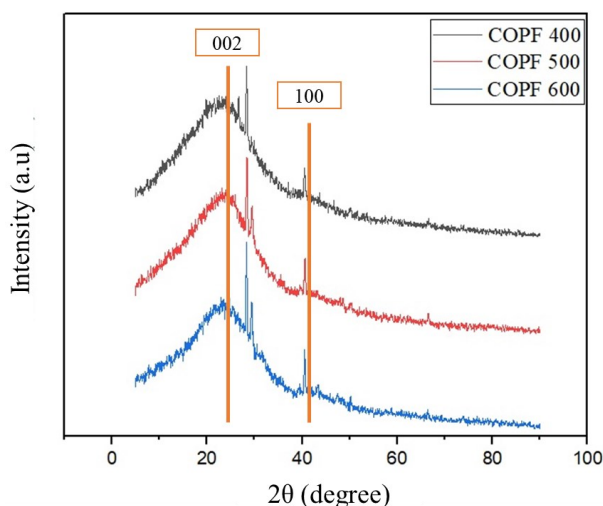


Figure 2. XRD diffractogram of COPF 400, COPF 500, and COPF 600

Figure 2 demonstrates that by increasing the carbonization temperature, the peak intensity of COPF 400, COPF 500, and COPF 600 increases at $2\theta = 22\text{--}25^\circ$ (2016.67; 2138.33, and 2158.33 $^\circ$) and $42\text{--}44^\circ$ (725.00, 791.66, and 783.33 $^\circ$). Increasing the degree of crystallinity implies increasing the number of crystalline phases with increasing carbonization temperature. This was also confirmed by the calculated values of 4.04%,

6.61%, and 7.17% of the crystallinity degree. The value of the crystallinity of this charcoal comes from the change in the amorphous carbon structure of the oil palm frond, which is subjected to heat treatment and produces a semi-crystalline graphite structure [13]. This crystallinity value certainly affects the adsorption efficiency of COPF.

Adsorption was closely related to surface area (porosity). Increased crystallinity can occur due to normal shrinkage in the crystallite structure of charcoal, which cause results in wider gaps between crystals and more pores. The porosity and surface area will increase along with the higher crystallinity, which causes the adsorption efficiency to increase [14]. This result was evidenced by the ratio data Lc (crystal height) and La (crystal width), shown in Table 2.

Table 2. Sample lattice parameters based on XRD results

Sample	2θ (002) ($^\circ$)	2θ (100) ($^\circ$)	Lc (nm)	La (nm)	Lc/La
COPF 400	22.845	42.669	8.061	24.123	0.334
COPF 500	23.927	43.692	8.427	23.529	0.358
COPF 600	24.204	43.734	8.587	21.055	0.407

In Table 2, the Lc/La ratio for COPF 400, COPF 500, and COPF 600 samples increased, indicating a greater surface area [15]. Higher Lc implies more bonding of carbon atoms, which causes the distance between layers and the width of the lattice layer (La) to decrease. The microcrystalline value is related to the surface area of the charcoal; when La decreases and Lc increases, the carbon surface area will be higher [14].

3.4. Surface morphology of COPF

The surface morphology of COPF was analyzed using Scanning Electron Microscopy (SEM). Figure 3 shows the surface morphology of COPF for each temperature variation (400, 500, and 600 $^\circ\text{C}$).

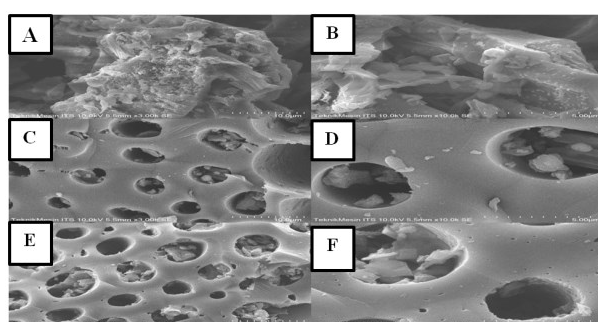


Figure 3. Surface morphology of COPF using SEM (ACE 3000 \times magnification, BDF 10,000 \times magnification)

The carbonization temperature causes differences in the size and shape of the surface pores of the synthesized charcoal. The pore sizes of each charcoal obtained from SEM analysis with ImageJ application were COPF 400 (5.71 microns), COPF 500 (4.37 microns), and COPF 600 (4.16 microns). In Figure 3, COPF 400 (A and B) has large pore sizes with irregular shapes and a lot of tar and ash covering the pores, thus reducing its adsorption efficiency. The pore size is much smaller, yet there are more pores at COPF 600 (E and F) than at COPF 500 (C and D).

The surface morphology of COPF 500 features relatively small pores with minimal tar and ash on them.

The COPF 600 surface has relatively more pores and is somewhat smaller than COPF 400 and 500 due to the difference in carbonization temperature. The number and size of the pores increase with the carbonization temperature. The higher thermal energy makes the particles move faster, increasing particle collisions and the number of pores produced. In addition, the heat penetrating the surface will damage the large pore structure, resulting in the formation of smaller pores [16]. The pore sizes of COPF 500 and COPF 600 are relatively similar, but the pores of COPF 600 are covered by more tar and ash. The higher the carbonization temperature and time, the higher the ash content formed. The ash can interfere with the adsorption process of charcoal because it covers the pores [9].

3.5. Initial peat water analysis

A sampling method from peat water was carried out based on SNI 6989.59-2008 (water and wastewater sampling method) and SNI 06-6989.4-2004 (method of testing for iron (Fe)) using the AAS instrument. Odor, pH, and initial Fe content in peat water were the first parameters identified from peat water sampling. Odor parameters were analyzed organoleptically by 12 respondents. Before and after the adsorption of peat water can be seen in Table 3.

Table 3. Characteristics of peat water before and after adsorption

Parameter	Before adsorption	After adsorption (COPF 500)
Odor*	Slight odor	Odorless
Color*	Dark chocolate	Colorless
peat water pH	3.10	7.10
Iron (ppm)	0.66	0.00

*data obtained from 12 respondents

3.6. Adsorption of Fe(III) from peat water

3.6.1. Effect of contact time

Figure 4 displays the results of Fe adsorption with various contact times. A 30-minute adsorption test revealed that COPF 400 had an adsorption efficiency of 94.76%, COPF 500 had the highest adsorption efficiency of 100%, and COPF 600 had the lowest adsorption efficiency of 96.13%. Adsorption for 15 minutes did not generate optimal results because the adsorbate was not equally distributed on the active site of the adsorbent, and collisions between the adsorbate and the active area of the adsorbent were unlikely. The rapid adsorption process resulted in an uneven distribution of adsorbent particles on the surface of the adsorbent [5].

The best adsorption activity was achieved with 30 minutes of contact time. It can be seen from the increase in Fe (III) adsorption and is the optimal point for adsorption. This may occur due to the increased contact time; the adsorbate may be equally distributed on the active site, and the likelihood of collision between the adsorbate and the active site rises. Increasing contact time results in more significant metal adsorption [15]. The adsorption efficiency decreased as the contact time increased from 30 minutes to 45 and 60 minutes. The number of unoccupied sites reduces with time, thus

resulting in a slower adsorption rate. When the adsorption sites are depleted, there is a repulsion between the adsorbate and the adsorbent's surface [5].

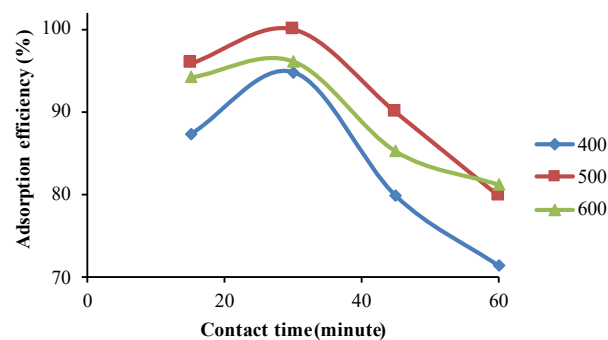


Figure 4. Graph of the relationship between contact time and the adsorption efficiency of Fe (III) at various carbonization temperatures

The decrease in adsorption efficiency can also be explained by the water and ash content. COPF 500 has a higher adsorption efficiency than COPF 400 because of its low water content. The remaining water in the substance can block the surface pores, blocking access to the active site [17]. Although COPF 600 has a lower water content than COPF 500, the higher ash content decreases its adsorption efficiency. High ash content can block the pores on the surface of the adsorbent, thus reducing its surface area. A material with a reduced ash content is more effective as an adsorbent [18].

The IR spectra of COPF 500 show a lower intensity than COPF 400 on the vibrations of the O-H and C-H functional groups, implying the functional groups in cellulose. The decrease in energy can be attributed to the thermal degradation of cellulose. The degradation of cellulose and other carbon compounds has resulted in forming of many pores of decreasing size. This result may also be explained by the degree of crystallinity. Increasing the degree of crystallinity improves the porosity and surface area in line with the Lc/La ratio value, which also increases the adsorption efficiency [14]. The degree of crystallinity increased from COPF 400, COPF 500, and COPF 600. According to these results, COPF 500 exhibits the highest adsorption capacity, followed by COPF 600 and COPF 400. COPF 600 contains more ash than COPF 500, thus reducing adsorption capacity. As depicted in Figures 3A and B, the surface morphology of COPF 500 has a relatively small pore size (4.37 microns), a rather large number of pores, and minimal combustion residue compared to COPF 400.

Based on the trend graph in Figure 4, which depicts the correlation between the adsorption efficiency of Fe (III) and various contact times, the optimum adsorption time is 30 minutes. This contact time was employed as reaction time in the second adsorption stage by varying the COPF mass.

3.6.2. Variation of adsorbent mass

It can be seen from Figure 5 the percentage of removal initially increased with increasing adsorbent mass but decreased after 1 g. COPF 500 had the best adsorption efficiency among the three materials, with 0.054 mg adsorbed using 1 g of adsorbent. The adsorption

efficiency increased from 0.5 g to 1 g because adding adsorbent mass increased the adsorbent surface area and available pores. The increase in adsorbent mass will cause more available active sites [19]. Hence, the optimum adsorbent mass for Fe(III) adsorption was 1 g.

The adsorption efficiency decreased from 1 g to 2 g because with the increase in the mass of the adsorbent and there would be aggregation on the adsorbent so that the surface area would decrease. There are more active sites at low adsorbent mass because adsorbent aggregation occurs with increasing adsorbent mass, and efficiency decreases [20]. The optimum adsorbent mass was obtained at an adsorbent mass of 1 g, according to the trend graph in Figure 5.

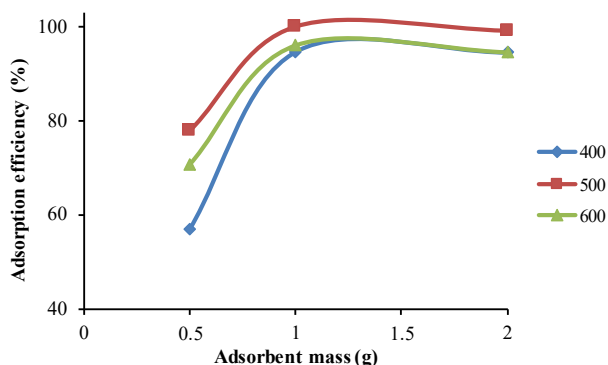


Figure 5. Graph of the relationship between adsorbent mass and adsorption efficiency of Fe (III) at various carbonization temperatures

3.6.3. Variation of peat water volume

COPF 500 has the highest efficiency of 100% in the adsorption of Fe(III) from peat water, with the best volume of 100 mL and an adsorbed mass of 0.054 mg. Figure 6 demonstrates that the adsorption efficiency of Fe(III) decreases as the volume increases from 100 mL to 300 mL. This decrease was caused by the increased interaction between adsorbate particles, thus making the active site challenging to access. Nevertheless, the adsorbate particles impede one another [21]. The optimum volume of peat water in this adsorption test was obtained at 100 mL by examining the trend graph in Figure 6. The comparison of the adsorption efficiency of Fe in other studies can be observed in Table 4.

Table 4. Comparison of the efficiency of Fe adsorption by COPF with other studies

No.	Type of adsorbent	Efficiency (%)	Reference
1	COPF 500	100	This research
2	Ca-Alginate	79.28	[7]
3	Chitosan membrane	92.20	[6]
4	Coffea Robusta Waste Active Carbon	65.40	[22]

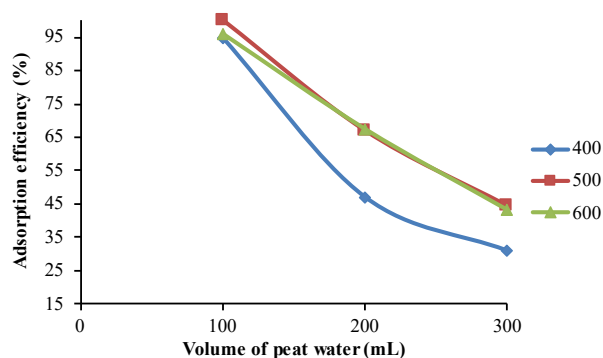


Figure 6. Graph of the relationship between the volume of adsorbate and adsorption efficiency of Fe (III) at various carbonization temperatures

4. Conclusion

The synthesized charcoal with various carbonization temperatures of 400, 500, and 600°C showed a water content that decreases with increasing temperature, with the highest water content of 3.78% obtained by COPF 400. Likewise, the ash content increases with increasing temperature, with COPF 600 producing the greatest ash content at 9.58%. Identification of functional groups on the surface of COPF indicated the presence of groups such as C-O, O-H, C=O, and C-H with differences in vibration intensity. Increasing the carbonization temperature reduces the pore size and increases the pore count. The degree of crystallinity grows as the carbonization temperature rises. Increasing the degree of crystallization results in a high Lc/La ratio, which implies an increase in surface area. The highest Fe(III) adsorption efficiency was obtained by COPF 500 with 30 minutes of contact time, 1 g of adsorbent mass, and 100 mL of peat water. The higher the water and ash content decreases the adsorption efficiency because the high water and ash content can cover the pores, thereby inhibiting the adsorption process.

References

- [1] Badan Pusat Statistik, *Statistik Kelapa Sawit Indonesia 2018*, Badan Pusat Statistik, Jakarta, 2018
- [2] S. Maulina, M. Iriansyah, Characteristics of activated carbon resulted from pyrolysis of the oil palm fronds powder, *IOP Conference Series: Materials Science and Engineering*, 2018 <https://doi.org/10.1088/1757-899X/309/1/012072>
- [3] Rananda Vinsiah, Andi Suharman, D. Desi, Pembuatan karbon aktif dari cangkang kulit buah karet (*hevea brasiliensis*), *Jurnal Teknik Kimia*, 6, 1, (2015), 189-199
- [4] Muhdarina Muhdarina, Nurhayati Nurhayati, Mhd Reza Pahlepi, Zetria Pujiana, Syaiful Bahri, Penyiapan Arang Aktif Pelepah Kelapa Sawit sebagai Adsorben Asam Lemak Bebas dari CPO (Crude Palm Oil), *al-Kimiya: Jurnal Ilmu Kimia dan Terapan*, 7, 1, (2020), 7-13 <https://doi.org/10.15575/ak.v7i1.6497>
- [5] Asih Melati, Galih Padmasari, Rama Oktavian, Frida A. Rakhmadi, A comparative study of carbon nanofiber (CNF) and activated carbon based on coconut shell for ammonia (NH₃) adsorption performance, *Applied Physics A*, 128, 3, (2022), 211 <https://doi.org/10.1007/s00339-022-05336-z>

- [6] Khadijah Lestari Lubis, Shinta Elystia, Dini Aulia Sari Ermal, Zultiniar Zultiniar, Penyisihan Logam Fe pada Air Gambut Menggunakan Membran Chitosan sebagai Adsorben: Removal of Fe From Peat Water Using Chitosan Membrane as Adsorbent, *Jurnal Sains Teknologi dan Lingkungan*, 8, 1, (2022), 15-24 <https://doi.org/10.29303/jstl.v8i1.298>
- [7] Elliska Murni Harfinda, Ca-Alginat untuk Adsorpsi Fe dan Mn pada Air Gambut, *Jurnal Kimia Mulawarman*, 18, 1, (2020), 16-21 <https://doi.org/10.30872/jkm.v18i1.844>
- [8] Ahmed Y. Elnour, Abdulaziz A. Alghyamah, Hamid M. Shaikh, Anesh M. Poulouse, Saeed M. Al-Zahrani, Arfat Anis, Mohammad I. Al-Wabel, Effect of pyrolysis temperature on biochar microstructural evolution, physicochemical characteristics, and its influence on biochar/polypropylene composites, *Applied Sciences*, 9, 6, (2019), 1149 <https://doi.org/10.3390/app9061149>
- [9] C. L. Lee, P. S. H'ng, M. T. Paridah, K. L. Chin, P. S. Khoo, R. A. R. Nazrin, S. N. Asyikin, M. Mariusz, Effect of reaction time and temperature on the properties of carbon black made from palm kernel and coconut shell, *Asian Journal of Scientific Research*, 10, 1, (2017), 24-33 <https://dx.doi.org/10.3923/ajsr.2017.24.33>
- [10] Noor Afeefah Nordin, Othman Sulaiman, Rokiah Hashim, Mohamad Haafiz Mohamad Kassim, Characterization of different parts of oil palm fronds (*Elaeis guineensis*) and its properties, *International Journal on Advanced Science, Engineering and Information Technology*, 6, 1, (2016), 74-76 <https://doi.org/10.18517/ijaseit.6.1.643>
- [11] Mohd Adib Yahya, Zakaria Al-Qodah, C. W. Zanariah Ngah, Agricultural bio-waste materials as potential sustainable precursors used for activated carbon production: A review, *Renewable and Sustainable Energy Reviews*, 46, (2015), 218-235 <https://doi.org/10.1016/j.rser.2015.02.051>
- [12] Ananias Francisco Dias, Renata Nunes de Oliveira, Xavier Deglise, Natália Dias de Souza, José Otávio Brito, Infrared spectroscopy analysis on charcoal generated by the pyrolysis of *Corymbia. citriodora* wood, *Matéria (Rio de Janeiro)*, 24, 3, (2019), 1-7 <https://doi.org/10.1590/S1517-707620190003.0700>
- [13] Saptadi Darmawan, Wasrin Syafii, Nyoman J. Wistara, Akhirudin Maddu, Gustan Pari, Kajian struktur arang-pirolisis, arang-hidro dan karbon aktif dari kayu *Acacia mangium* Willd. menggunakan difraksi sinar-x, *Jurnal Penelitian Hasil Hutan*, 33, 2, (2015), 81-92 <https://doi.org/10.20886/jphh.2015.33.2.81-92>
- [14] Rakhmawati Farma, Physical Properties Analysis of Activated Carbon From Oil Palm Empty Fruit Bunch Fiber on Methylene Blue Adsorption, *Journal of Technomaterial Physics*, 1, 1, (2019), 67-73 <https://doi.org/10.32734/jotpv1i1.824>
- [15] Panda H., N. Tiadi, M. Mohanty, C. R. Mohanty, Studies on adsorption behavior of an industrial waste for removal of chromium from aqueous solution, *South African Journal of Chemical Engineering*, 23, 1, (2017), 132-138 <https://doi.org/10.1016/j.sajce.2017.05.002>
- [16] Thanchanok Pagketanang, Apichart Artnaseaw, Prasong Wongwicha, Mallika Thabuot, Microporous activated carbon from KOH-activation of rubber seed-shells for application in capacitor electrode, *Energy Procedia*, 79, (2015), 651-656 <https://doi.org/10.1016/j.egypro.2015.11.550>
- [17] Pei-Hsing Huang, Shih-Han Chen, Effect of moisture content, system pressure, and temperature on the adsorption of carbon dioxide in carbon nanotube and graphite composite structures using molecular dynamics simulations, *Journal of Nanoscience and Nanotechnology*, 16, 8, (2016), 8654-8661 <https://doi.org/10.1166/jnn.2016.11784>
- [18] O. A. Ekpete, A. C. Marcus, V. Osi, Preparation and characterization of activated carbon obtained from plantain (*Musa paradisiaca*) fruit stem, *Journal of Chemistry*, 2017, 8635615, (2017), 1-7 <https://doi.org/10.1155/2017/8635615>
- [19] Fatemeh Gorzin, M. M. Bahri Rasht Abadi, Adsorption of Cr (VI) from aqueous solution by adsorbent prepared from paper mill sludge: Kinetics and thermodynamics studies, *Adsorption Science and Technology*, 36, 1-2, (2018), 149-169 <https://doi.org/10.1177/0263617416686976>
- [20] K. S. Padmavathy, G. Madhu, P. V. Haseena, A study on effects of pH, adsorbent dosage, time, initial concentration and adsorption isotherm study for the removal of hexavalent chromium (Cr (VI)) from wastewater by magnetite nanoparticles, *Procedia Technology*, 24, (2016), 585-594 <https://doi.org/10.1016/j.protcy.2016.05.127>
- [21] Abdulaziz Ali Alghamdi, Abdel-Basit Al-Odayni, Waseem Sharaf Saeed, Abdullah Al-Kahtani, Fahad A. Alharthi, Taieb Aouak, Efficient adsorption of lead (II) from aqueous phase solutions using polypyrrole-based activated carbon, *Materials*, 12, 12, (2019), 2020 <https://doi.org/10.3390/ma12122020>
- [22] Sri Ayu Emy Istighfarini, Syarfi Daud, Edward Hs, Pengaruh massa dan ukuran partikel adsorben sabut kelapa terhadap efisiensi penyisihan Fe pada air gambut, *Environmental Engineering, Riau University, Riau*, 2017